Contents lists available at ScienceDirect

Arabian Journal of Chemistry

journal homepage: www.ksu.edu.sa

Kinetic verification and Comsol modeling of the Diels-Alder reaction of conjugated pentadiene with maleic anhydride in a continuous flow capillary reactor

Lei Yin [a], Tingting Ge [a], Cuncun Zuo [a,*], Ming Wang [a], Guangjun Cui [b], Yuchao Li [a], Haofei Huang [a,*], Liping Zhang [c]

[a] Research Institute of Clean Chemical Technology, School of Chemistry and Chemical Engineering, Shandong University of Technology, Zibo 255049, People's Republic of China
[b] Institute of Zibo Luhua Hongjin New Material Group Co., Ltd. and Clean Chemical Technology, School of Chemistry and Chemical Engineering, Shandong University of Technology, Zibo 255000, People's Republic of China
[c] Zibo Interenergy technology Ltd,.Co., Zibo 255000, People's Republic of China

ARTICLE INFO

Keywords:
Continuous flow capillary reactor
Strong exothermic reaction
Mass balance
Kinetic
Comsol modeling

ABSTRACT

Synthesis of 3/4-methyltetrahydrophthalic anhydride was carried out by the Diels-Alder reaction in a continuous flow capillary reactor. The efficient liquid–liquid reaction of pentadiene with molten maleic anhydride provided a theoretical basis for replacing the conventional batch reaction process. Different inner diameter sizes of the channel tubes were adjusted in the range of 0.50 ~ 2.00 mm to find the optimal size to match the strong exothermic reaction. Under the capillary channel size of 0.8 mm, the conversion rate of C5 and MA reached 100 % when n_{C5}: n_{MA} = 1.08:1 at 65 °C for 8 min. The D-A reaction process is accompanied by the autopolymerization of diolefin in the batch reactor. Our results showed that choosing a continuous flow capillary reactor of appropriate size can directly improve the selectivity of the reaction and the quality of the product. The accurate reaction rate constant and activation energy were obtained by establishing a kinetic model, and the effects of temperature, reaction time and pipe diameter were designed using Comsol software.

1. Introduction

Methyl tetrahydrophthalic anhydride (MTHPA) (Wazarkar and Sabnis, 2018; Kadhim et al., 2024; Barabanova et al., 2019; Abid and Kadhim, 2020) is a mixture of 3-MTHPA and 4-MTHPA, which can be modified by isomerisation reaction to become an excellent curing agent for organic anhydrides of liquid epoxy resins. The application of this type of curing agent is developing rapidly with the increasing requirements for the reliability of insulating structures in the aerospace, electronics, and electrical industries. (Saeedi et al., 2019; Wang et al., 2019a; Zhang et al., 2023; Abideen et al., 2020; Ul Abideen and Teng, 2018; Zhang et al., 2018) The traditional synthesis method was to use an intermittent reactor to slowly add maleic anhydride (MA) dropwise to diene, and perform Diels-Alder (D-A) reaction under certain conditions. (Salih et al., 2024; Medrán et al., 2019; Briou et al., 2021) Continuous process has become a common means for enterprises to pursue higher yield, and tubular reactor has become the research direction of D-A reaction with C_5 and MA liquid feed.

D-A reaction is one of the most widely used and effective synthesis methods of six-membered ring materials at present, but it is also a strongly exothermic reaction. When the heat transfer is not enough, the self-polymerization of olefin will be caused, which will affect the quality and stability of the product. (Girish et al., 2017) The anhydride curing agent (MTHPA) containing a six-membered ring was prepared by D-A reaction of MA and mixed C_5, but the pyrolysis of C_5 has a lower boiling point, which causes it to evaporate into a gas phase at slightly higher temperatures. (Hou et al., 2022) C_5 was prone to self-polymerization during phase transformation. To ensure a homogeneous D-A reaction, pressure should be increased, and reaction rate should be increased in a homogeneous system. (Fedyaeva et al., 2019) In the kettle reactor, the addition rate of MA needs to be strictly controlled, too fast adding causing irreversible self-polymerization side reactions due to fly temperature for instantaneous reactions, and too slow adding reducing production efficiency, which makes it hard to produce continuously and

* Corresponding authors.
E-mail addresses: zcc_xtu@163.com (C. Zuo), 1982hhf@163.com (H. Huang).

https://doi.org/10.1016/j.arabjc.2024.105696
Received 12 November 2023; Accepted 23 February 2024
Available online 24 February 2024

difficult to guarantee the product quality due to the strong exothermic characteristics of D–A reaction. (Nguyen et al., 2019; Abid and Kadhim, 2022; Sheehan and Sharratt, 1998; Ma et al., 2019) Using a continuous flow capillary reactor in a D-A reaction was a promising and effective method to avoid this situation. (Yan et al., 2020).

In recent years, to overcome the problem of mass transfer and heat transfer, microreactors have been widely used. With its unique microstructure, the microreactor successfully solves the problems that the traditional reactor is difficult to control temperature and easy to explode. (Pennemann et al., 2004; Sagandira et al., 2020; Pontes et al., 2016; Asano et al., 2019; Liu et al., 2022) Many types of chemical reactions have realized the application of microchannel reactors, such as nitration (Russo et al., 2017; Deng et al., 2017), Catalytic hydrogenation reaction (Cao and Noël, 2019; Ion and Faïçal, 2023; Jean and d. S., José, L. F. A., Guilherme, D. M., Michele, D. D., , 2023), Low-temperature reaction (Shuai et al., 2022), Oxidation reaction (Zhou et al., 2022; Inoue et al., 2013; Yun et al., 2021), Bromination, chlorination (Wan et al., 2022; Wan et al., 2020) and fluorination reaction (Fu et al., 2021), Cyclization reaction (Mizuno et al., 2016), Diazotization reaction (Deng et al., 2017; F. J. Wang et al., 2019b; Wang et al., 2018), etc. Carmela De Risi et al. (De Risi et al., 2020) summarized the application of D-A reaction in microreactors, and bicyclononyne- polylactic acid (BCN-PLA) and tetrazine-PLA block copolymers were further functionalized by the inverse electron demand Diels-Alder (IEDDA) reaction, providing new PLA materials for biomedical and other applications. In the Diels-Alder reaction of cyclopentadiene and e-cinnamaldehyde, the cumulative yield of the reaction's internal and external adduct increases with the reaction time, but the continuous flow capillary reactor has better enantioselectivity for each monomer. The yield is increased from 50 % of batch reactor to 80 % of microreactor, and the flow strategy resulted in microreactor having an advantage in terms of catalytic activity, whereas in batch there was an irreversible loss of catalyst activity.

The complex multiphase behavior and control factors of microchannel reactors need further study, especially in the preparation of fine chemical products, which will bring efficient development to the chemical industry. (de Oliveira et al., 2019; Abiev et al., 2019; Yuichi et al., 2022; Aguilar et al., 2020) Many researchers are studying the synthesis and application of microreactors, and have some theoretical calculations as support. (de Oliveira et al., 2020; Chen et al., 2017; Santana et al., 2016) However, the key was the lack of research on the modeling, simulation, and optimization of microreactors. Several researchers have successfully modeled and simulated the reaction process using Comsol and Ansys simulation software, accurately explaining the complex changes in mass transfer, heat transfer, momentum, and reaction engineering in continuous flow capillary reactors, and quantifying these microscopic phenomena.(Yedala and Kaisare, 2021).

In our past studies, the differences between 3/4-MTHPA have been discussed in detail with ^{1}H NMR and FT-IR. (Yin et al., 2023) In this study, 3/4-MTHPA was synthesized with isoprene / 1, 3-pentadiene and MA in a homogeneous Diels-Alder reaction using continuous flow capillary reactor of different sizes (0.50 ~ 2.00 mm). By discussing the influence factors of the experiment, the temperature was determined to be 65 ℃, the residence time was 8 min and the material ratio was n_{C5}: n_{MA} = 1.08:1. Orthogonal experiments were designed to find the optimal size matching the strong exothermic reaction of 0.5 ~ 0.8 mm. At the same time, in order to avoid the evaporation of pentadiene during the reaction and the destruction of the continuous homogeneous reaction system, the appropriate reaction pressure was obtained by Aspen simulation. The experimental data and kinetic equations fit well, which proves that the microreactor can optimize the D-A reaction and avoid the occurrence of side reactions. Based on the experimental results, a Comsol flow model was established to simulate the reaction.

2. Experimental

2.1. Materials

MA (≥99.5 %), Catechol (as polymerization inhibitor, ≥99 %), were purchased from Sinopharm Chemical Reagent Co., LTD. Mixed C_5-diolefin: the total mass fraction of m-pentadiene and isoprene accounted for about 55 % (the rest were inactive components), MTHPA (≥95 %) was supplied by Zibo Luhua Hongjin Research Institute; All the chemicals are analytical grade and have not been further purified.

2.2. Equipment

The WZD100ml high-temperature and high-pressure reactor produced by Beijing Wuzhou Dingchuang Co., Ltd. The 2 PB-3020IV horizontal flow pump produced by Beijing Xingda Technology Co., Ltd. The heating tank and JRZ-10020CH CRH high-temperature heating pump produced by Hangzhou Jingjin Technology Co., Ltd. PTFE Y-shaped tee produced by Nanjing Runze Fluid Control Equipment Co., Ltd. DF-101S collector constant temperature magnetic stirrer produced by Shanghai Lichen Bonsai Instrument Co., Ltd.

Agilent gas chromatograph analysis, the chromatographic column was PONA type quartz capillary column (φ 0.2 mm × 0.5 μm × 50 m), FID detector; NEXUS470 infrared spectrometer (American thermoelectric company); AVANCEIII 500 MHz Fully digital Fourier Superconducting ^{1}H NMR spectrometer (Bruker, Switzerland).

2.3. Experimental process

Batch reaction: added MA into reactor, fill 0.3 MPa nitrogen, and heated it to melt at 50 °C. Pumped C_5 slowly into reactor at a flow rate of 0.4 mL/min for a reaction for some time. After reaction, the surplus C_5 was separated by rotating evaporation at 40 °C. The experimental process was shown in Fig. 1.

Continuous flow capillary reactor reaction: Maleic anhydride was melted with a melt bath, measured, and transported with a heating pump. All pipes carrying MA required an electric heating belt to prevent solidification. C_5 was pumped into a Y-type continuous flow capillary reactor at a specific flow rate. The heat pump and heat belt temperature was set to 50 ~ 80 °C. Different-diameter continuous flow capillary reactor were coupled to a Y-type three-way mixer. High-precision external circulation thermostatic water bath was used to precisely control the mixer and reactor, and the back pressure valve at the reactor's output was used to control pressure. The experimental process was shown in Fig. 2.

2.4. Analysis method

The samples were analyzed qualitatively and quantitatively by gas chromatography. The gas chromatography configuration is a capillary column (Agilent-8860; flame ionization detector (FID) and HP-5 column (30 m × 320 μm × 0.25 μm). The experimental results were subject to the percentage content of MA calculated by Eq. (1).

$$N = \frac{n_{MTHPA}}{n_{MA} + n_{MTHPA}} \times 100\% = \frac{S_{MTHPA}/166}{S_{MA}/98 + S_{MTHPA}/166} \quad (1)$$

N: Conversion; *S*: Peak area; 98/166: Relative molecular mass of MA/MTHPA.

2.5. Comsol modeling

The running-in of the Y-shaped channel with the experimental size, mesh refinement, and experimental error reduction were all achieved using Comsol modeling. The reaction was configured to run in adiabatic mode during the modeling design. The pressure drop of continuous flow

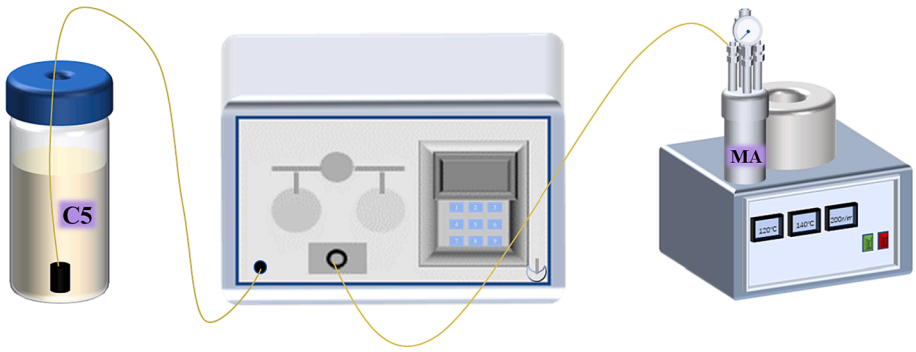

Fig. 1. Kettle reaction experimental process.

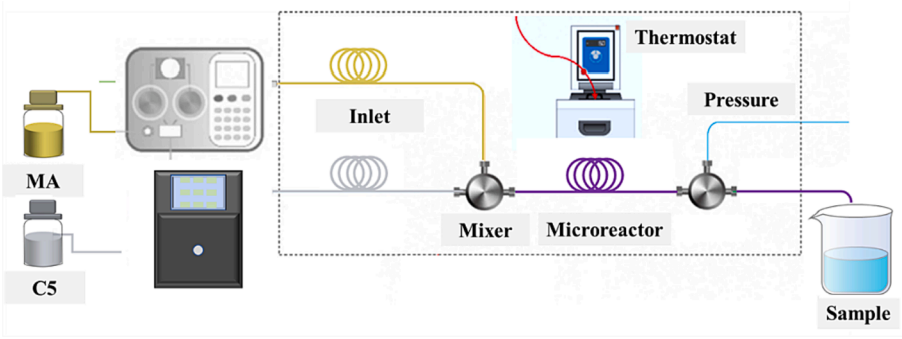

Fig. 2. Continuous flow capillary reactor experimental process.

capillary reactor can be disregarded because it was assumed that the mixture was a uniform Newtonian fluid and an incompressible fluid. The reaction part of the Y-type mixed continuous flow capillary reactor was a coil with a diameter of 0.5 ~ 2.0 mm, and it was made up of two parts: two straight pipes with a 2 cm intake. The specific model was shown in Fig. 3.

The units and physical quantities designed in the Comsol modeling process was summarized, including (2) strong coupling of the reaction process, partial differential equations of fluid mechanics, mass transfer and production, (3) dilute matter transfer equation, (4) chemical reaction equation, (5) turbulent momentum and continuity equation and (6) Reaction rate equation. The physical quantities used were shown in Table 1.

$$\rho\frac{\partial u}{\partial t}+\rho(u\hat{\mathrm{A}}\cdot\nabla)\mathrm{u}=-\nabla\mathrm{p}+\nabla\hat{\mathrm{A}}\cdot\left(\eta\left[\nabla\mathrm{u}+(\nabla\mathrm{u})^{T}\right]\right),\ \nabla\hat{\mathrm{A}}\cdot u=0 \tag{2}$$

$$\nabla\hat{\mathrm{A}}\cdot J_i+u\hat{\mathrm{A}}\cdot\nabla C_i=R_i, J_i=-D_i\nabla C_i \tag{3}$$

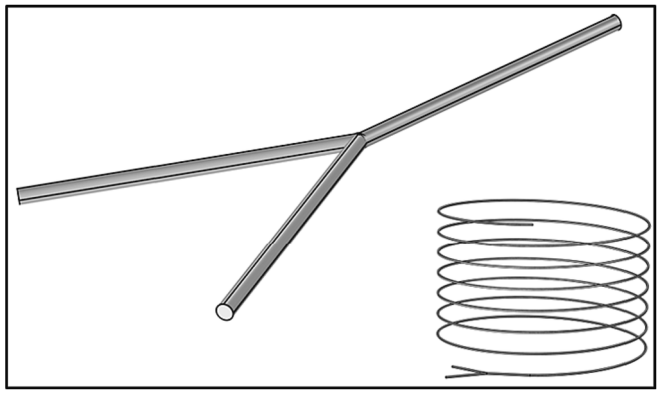

Fig. 3. Y-type continuous flow capillary reactor modeling.

Table 1
Relevant physical property parameters used in modeling process.

Physical quantity	Numerical value	Physical quantity	Numerical value
A	1.64×10^{4} m^3/(s·mol)	Ea	5.1×10^{4} J/mol
M_{C5}	0.068 kg/mol	ρ_{C5}	720 kg/m^3
M_{MA}	0.098 kg/mol	ρ_{MA}	1210 kg/m^3
M_{MTHPA}	0.166 kg/mol	ρ_{MTHPA}	1240 kg/m^3
M_{C5H12}	0.072 kg/mol	ρ_{C5H12}	620 kg/m^3
$C_{0,C5}$	232.4 mol/m^3	$C_{0,C5H12}$	192.5 mol/m^3
$C_{0,MA}$	207.4 mol/m^3	P	0.3 MPa
T	65 °C	ρ	1135 kg/m^3
μ(25 °C)	0.04 Pa·s	u_1	0.021 m/s
u_2	0.009 m/s	order of reaction	2

$$R_i=\sum_j R_{ij}, V_r\frac{dC_i}{dt}=V_rR_i \tag{4}$$

$$\rho\frac{\partial u_2}{\partial t}+\rho(u_2\hat{\mathrm{A}}\cdot\nabla)u_2=\nabla\hat{\mathrm{A}}\cdot[-P2_i+K]+F, \rho\nabla\hat{\mathrm{A}}\cdot u2=0 \tag{5}$$

$$C5+MA\xrightarrow{k}MTHPA, R=kC_{C5}\hat{\mathrm{A}}\cdot C_{MA} \tag{6}$$

3. Results and discussion

3.1. Characterization analysis

In our previous work, we made specific analysis of 3-MTHPA, 4-MTHPA, and 3/4 MTHPA, determined the difference of C = C–H chemical shift in ^{1}H NMR, and also determined the wavelength of each functional group in FT-IR, and had a clear understanding of MTHPA.

3.2. D-A synthesis reaction in batch reactor and continuous flow capillary reactor

3.2.1. Influence of pipe diameter on mass transfer efficiency

Four kinds of polytetrafluoroethylene (PTFE) pipes with inner diameters of 0.5, 0.8, 1.6 and 2.0 mm and tube lengths of 2.50, 2.48, 2.44 and 0.39 m, respectively, were used to investigate the effects of pipe diameter and residence time on D-A reaction. The reaction parameters were set to 65 °C, 0.3 MPa pressure, and n_{C5}: n_{MA} = 1.08:1, and the rest were listed in Table 2. On MA conversion, the consequences of D-A reaction at 8.06, 5.37, 4.13, 3.16, 1.07, and 0.534 min were debated. From Fig. 4, it can be seen that the pipe diameter has a great impact on the synthesis of MTHPA. The finer the microtubule, the larger the material contact area, the higher the mass transfer efficiency, and the higher the reaction conversion rate. The most suitable pipe diameter was 0.5 ~ 0.8 mm, but considering that the smaller the pipe diameter during the experiment, the smaller the feed speed, which is easy to cause fluctuations in the experimental data, 0.8 mm was chosen as the microchannel size. The conversion rate of reaction rapidly grew as residence time increased, and it might reach 100 % in 8 min.

The total volume mass transfer coefficient k_{La} was used to represent the rate of mass transfer, as shown in equation (7), where c* is the equilibrium concentration of MA at the outlet. The calculation results of the total mass transfer coefficient of each pipe diameter were shown in Table 3. It can be seen that with the increase of pipe diameter, the total mass transfer coefficient significantly decreases, and the strengthening effect of micro-size on mass transfer efficiency is significantly enhanced.

$$K_{La} = \frac{Q}{V}\int_{c_0}^{c_i}\frac{-dc}{c-c^*}$$

$$c^* = K_{rA}(c_B)^2 \tag{7}$$

3.2.2. Comparison between the kettle and continuous flow capillary reactor

C_5 and MA were used to synthesize 3/4-MTHPA in batch reactor and continuous flow capillary reactor. The experimental results were shown in Fig. 5. When conducting a D-A reaction in continuous flow capillary reactor, a reaction temperature lower than 55 °C will cause MA to solidify and block the pipeline. When conducting a D-A reaction in kettle reactor, a temperature higher than 75 °C will promote the polymerization reaction and product will become viscous and deteriorate.

At 65 °C, n_{C5}: n_{MA} = 1.08:1 to prepare MTHPA, and the conversion rate reached 100 % in the continuous flow capillary reactor for 8 min, which was far better than 98.42 % of that of kettle reactor for 10 min, but batch reactor's reaction took 30 min.

At the same time, the influence of raw material ratio in different reactors on D-A reaction was examined. The conversion rate of continuous flow capillary reactor was 100 % after 5.37 min reaction at 65℃ and n_{C5}: n_{MA} = 1.08:1, while the conversion rate of the reactor was only 98.94 % after 30 min reaction at this condition.

Table 2
Experimental conditions of continuous flow capillary reactor.

d (mm)	material	residence time (min)					
		8.06	5.37	4.13	3.16	1.07	0.54
0.5	Q_{C5} (ml/min)	0.170	0.255	0.339	0.434	1.275	2.550
	Q_{MA} (ml/min)	0.070	0.105	0.140	0.179	0.525	1.050
0.8	Q_{C5} (ml/min)	0.430	0.645	0.860	1.075	3.225	6.450
	Q_{MA} (ml/min)	0.180	0.270	0.360	0.450	1.350	2.700
1.2	Q_{C5} (ml/min)	0.960	1.440	1.915	2.400	7.200	14.400
	Q_{MA} (ml/min)	0.410	0.615	0.820	1.025	3.075	6.150
2.0	Q_{C5} (ml/min)	0.430	0.645	0.860	1.075	3.225	6.450
	Q_{MA} (ml/min)	0.180	0.270	0.360	0.450	1.350	2.700

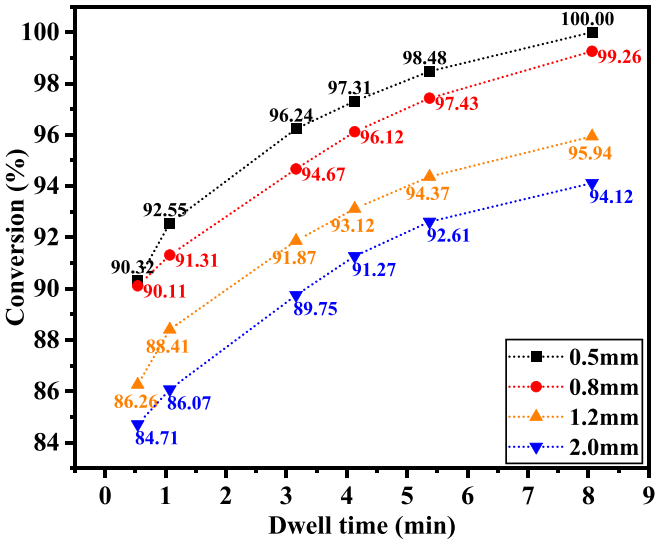

Fig. 4. Effects of different pipe diameters and different residence times on D-A reaction.

Table 3
Total mass transfer coefficient of each pipe diameter.

diameter	k_{La}	diameter	k_{La}
0.5	0.01436	0.8	0.01171
1.2	0.00938	2.0	0.00713

This study demonstrated that the micron-to-millimeter size structural channel in continuous flow capillary reactor had significantly increased the contact area and realized a significant increase in mass transfer and heat transfer efficiency, and easily break the restriction that the reaction speed of kettle reactor will gradually slow down even if the drip time of 50 min is ignored.

3.2.3. Kinetics correlation

The kinetics of the D-A reaction between C_5 and MA has been recognized by many scholars, and its second-order reaction kinetics equation was shown in Equation 8. In our previous work, (Jing et al., 2023) the kinetics of the D-A reaction was fully debated, and the reaction activation energy (Ea) of MTHPA was 50 ~ 55 kJ/mol and the pre-exponential factor (A) was 1.2 ~ 1.8 × 10^5. While the continuous flow capillary reactor optimized the reaction conditions and avoided the occurrence of polymerization side reactions, we verified it with the most basic kinetic formula and obtained excellent results.

The kinetics of reactor synthesis of MTHPA has been discussed for a long time, and the MTHPA reaction rate constant obtained by Lei Hao et al in China was 0.10587 $L{\cdot}mol^{-1}{\cdot}min^{-1}$, which was close to the reaction rate constant obtained by sampling calculation in our reactor synthesis process. Compared with the 0.5 ~ 0.8 mm microchannel reactor, the microsize can significantly improve the reaction rate.

$$y = \ln\left[\frac{b(a-x)}{a(b-x)}\right] \tag{8}$$

Table 4 showed the reaction rate constants when the microchannel was 0.5, 0.8, 1.2, and 2.0 mm. Fig. 6 confirmed that the calculated results of the second-order kinetics of D-A reaction under different pipe diameters and residence times were in good agreement with the experimental results. The experiments of the synthesis reaction at the microscale were in strict agreement with the theoretical calculation, which showed that the D-A reaction in the capillary can avoid the side reaction of diene autopolymerization..

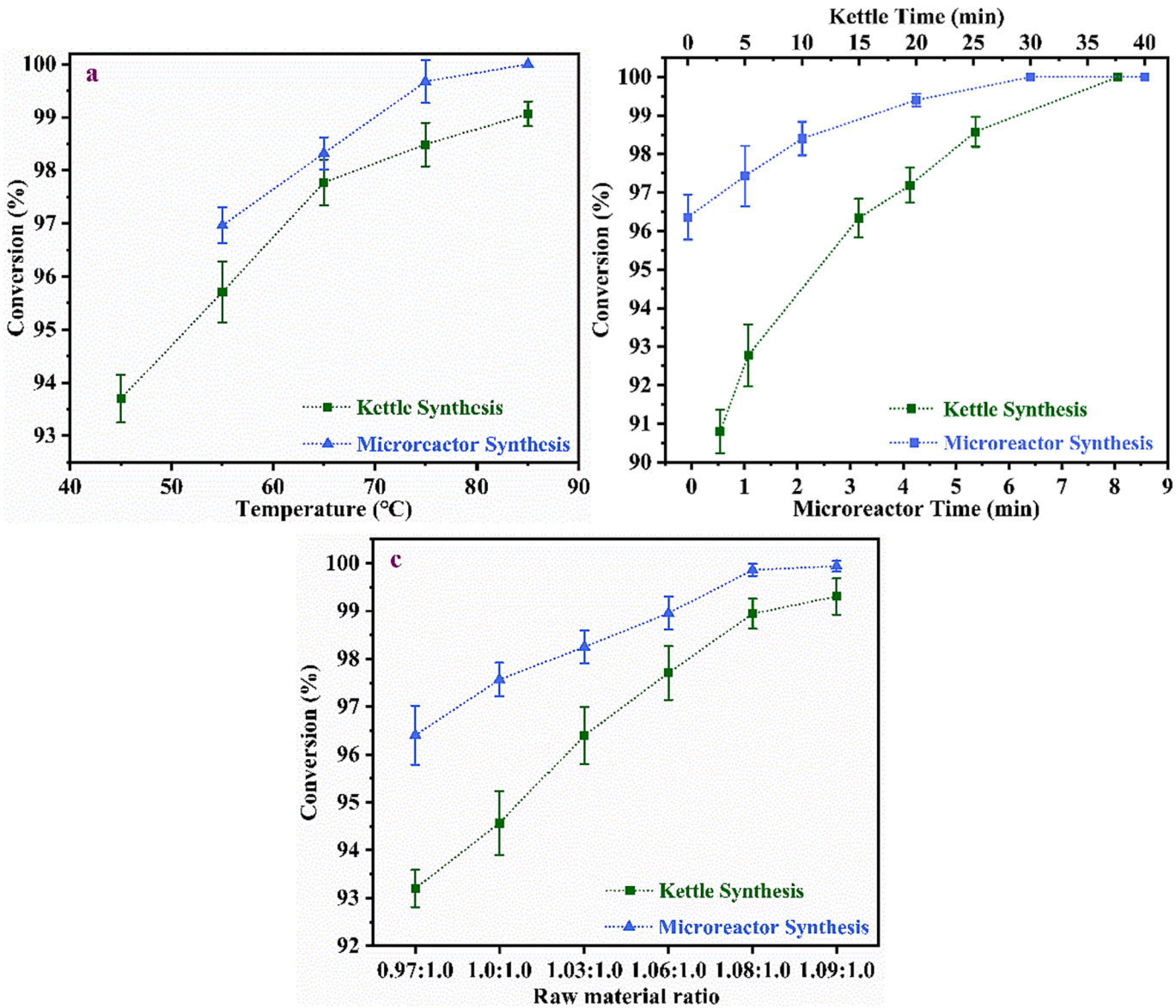

Fig. 5. Effects of different variables on MA conversion: (a) temperature (molar ratio = 1.06, the residence time of microreator = 5.37 min, the reaction time of kettle reactor = 30 min); (b) Time (temperature = 65 °C; molar ratio = 1.08); (c) Molar ratio (temperature = 65 °C, the residence time of microreator = 5.37 min, the reaction time of kettle reactor = 30 min).

Table 4
K and r^2 in different microchannels.

Pipe Diameter (mm)	k ($L \cdot mol^{-1} \cdot min^{-1}$)	R^2
0.5	0.25445	0.99962
0.8	0.24029	0.99938
1.2	0.08413	0.99938
2.0	0.05836	0.99959

3.2.4. Pressure calculation

As shown in Fig. 7, to ensure a homogeneous reaction, used Aspen to simulate the relationship between the saturated vapor pressure and temperature of piperylene and isoprene and determined that the pressure of the reaction system should be kept at 0.3 ~ 0.5 MPa at 65 °C. The Antoine equation was simulated and calculated as shown in Eq. (8).

$$lgp^{\circ} = -\frac{115.142}{t + 0.3} \tag{8}$$

In actual industrial production, the synthesis of MTHPA in the kettle reactor is usually protected with 0.3 MPa nitrogen, because the anaerobic and anhydrous synthesis conditions can reduce side reactions such as oxidation. Aspen fitting results indicated that 0.3 MPa low pressure protection should be adopted in order to prevent both vaporization and self-polymerization of C_5. Therefore, 0.3 MPa was the best system pressure for this reaction.

3.2.5. Orthogonal experimental

A quadratic mathematical model for each response was developed using the least squares error method. Table 5 showed the response variables. As shown, all responses followed a quadratic polynomial model. The model predicted the response values and compared them with the observed values, and the comparison of each response was shown in Fig. 8.

It can be seen from the response surface that the ideal MTHPA synthesis condition in 0.8 mm pipe diameter is: 75 °C, 6 min, C_5:MA = 1.05:1. Increasing the temperature did speed up the reaction process and even optimize the ratio of raw materials. However, in the actual experiment, we encountered a series of problems such as oxidation and

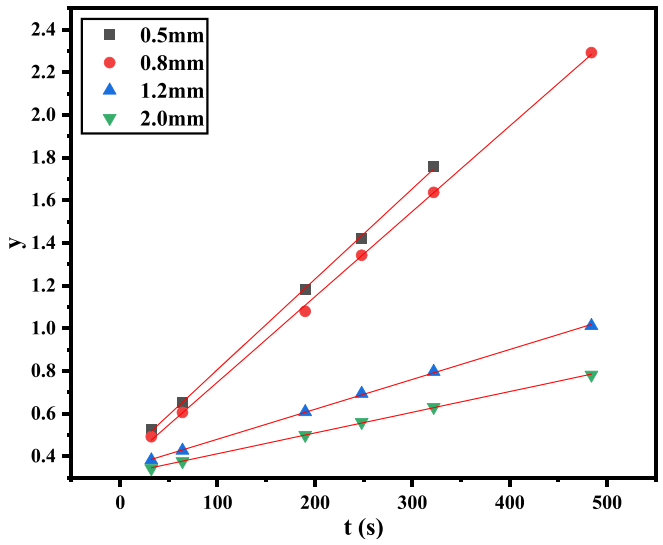

Fig. 6. Simulation of synthesis kinetics of different microchannels.

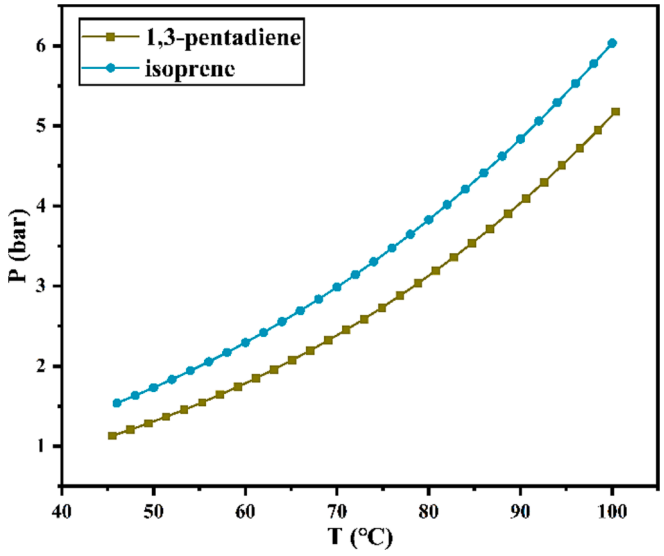

Fig. 7. Fitting results of saturated vapor pressure of 1, 3-pentadiene and isoprene.

hydrolysis of MA melted at high temperature for a long time, and side reactions led to pipeline blockage. Therefore, we previously selected 65 °C as a milder reaction condition and carried out reasonable experimental optimization.

3.2.6. Mass balance

Since the polymerization side reactions were avoided during the D-A reaction in the continuous flow capillary reactor, to ensure the correctness of the experimental results, we conducted a discussion of the changes of C_5, MA, and MTHPA concentrations at different residence time by controlling the flow rate. The mass equilibrium results were shown in Fig. 9. The impurities of raw material C_5 were alkanes and olefins, and there was no competitive reaction. The use of microchannel reactor and the optimization of conditions successfully avoided side reactions such as self-polymerization. The D-A reaction of pentadiene and MA was irreversible with stoichiometric number 1:1, and the material conservation of the system was only related to pentadiene, MA and MTHPA. As the concentration of C_5 and MA decreased, the concentration of MTHPA gradually increased until the reaction was in equilibrium.

Table 5
Orthogonal experiments on the factors affecting the conversion rate in continuous flow capillary reactors.

Temperature (°C)	Residence time (min)	C_5: MA ratio	Conversion (%)
70	4.5	1.05	95.88
70	4.5	1.05	95.88
80	4.5	1	92.44
80	1	1.05	89.31
80	8	1.05	99.28
70	8	1.1	100
80	4.5	1.1	97.13
70	4.5	1.05	95.88
70	4.5	1.05	95.88
70	1	1.1	85.45
70	4.5	1.05	95.88
70	1	1	78.11
60	8	1.05	90.65
60	4.5	1	79.37
70	8	1	96.24
60	4.5	1.1	86.07
70	4.5	1.05	95.88
70	4.5	1.05	95.88
60	1	1.05	72.22
70	4.5	1.05	95.88

3.3. CFD simulation

The D-A synthesis of pentadiene and MA was simulated by Comsol modeling software. The MA conversion results were shown in Fig. 10. The highest numerical conversion obtained was 100 % (temperature 75 °C, time 10 min, molar ratio 1.08).

Through simulation calculation, it can know that when the initial concentration C_5 = 232.4 mol/m^3, MA = 207.4 mol/m^3, the MA conversion rate can reach 98.68 % at 65 °C, while the conversion rate of reaction at 75 °C was as high as 99.78 %. The calculation time was deliberately extended to 10 min, and it was found that the conversion rate reached 100 % at 75 °C, while the conversion rate of reaction at 55 °C was as low as 96.74 %. Accurate kinetic parameters guided modeling and response surface analyses with very similar results, both reflecting that 75 °C is the best temperature choice for MTHPA synthesis, but considering the practical situation, 65 °C is favorable in terms of energy consumption and experimental stability.

The reaction length of the model was 2.2 m, which was consistent with the 2.0 ~ 2.5 m long microchannel applied in the experiment. After the calculation of reaction, mass transfer and fluid dynamics equations, the model simulation results of Comsol were shown in Fig. 11. It can see intuitively in the figure that although D-A reaction was rapid, with the extension of the pipeline, the product MTHPA had a significant concentration change. This was consistent with our calculation during the experiment. Increasing the flow rate or shortening the tube length would greatly reduce the conversion rate. The flow of fluid was continuous, and its flow velocity profile in the microchannel also told us that D-A reaction with fast reaction and strong exothermic in the continuous flow capillary reactor was very stable.

To determine the effect of pipe diameter on D-A reaction, the D-A reaction of PTFE microtubules used in the experiment was calculated under different diameters on Comsol software. The reaction conditions were fixed at 65 °C, 0.3 MPa, the residence time was 10 min, and the ratio of C_5 to MA was 1.08:1. The simulation results were shown in Fig. 12. In line with the experimental results, the conversion rate of 0.5 mm tube can easily reach 100 %, and the effect of 0.8 mm tube can also reach 99.5 %. With the increase of the diameter of the tube, the simulation results of the decrease of the conversion rate were in good agreement with the experimental law.

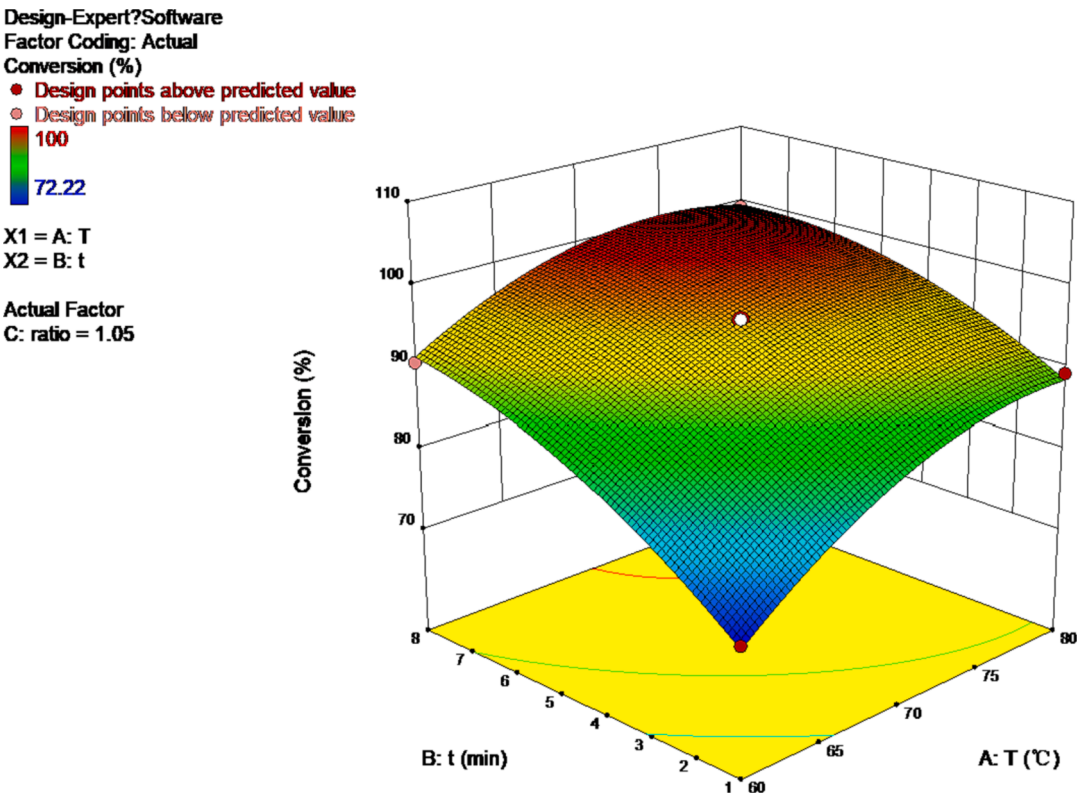

Fig. 8. Response surface simulation of temperature, residence time, and feedstock ratio for the D-A reaction.

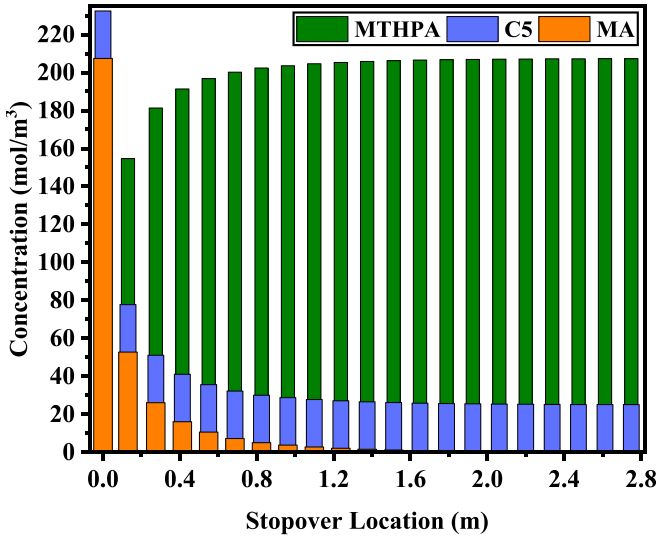

Fig. 9. Mass balance of C_5, MA, and MTHPA concentrations at different staying cross section.

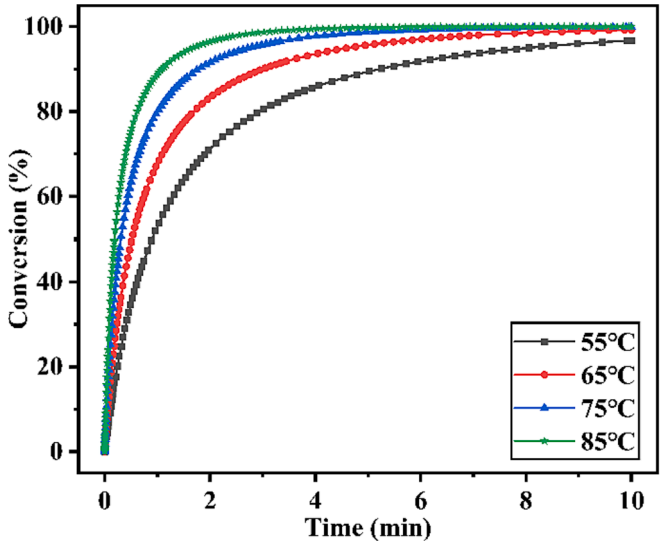

Fig. 10. Simulation of reaction conditions of continuous flow capillary reactor.

3.4. Qualitative comparison between experimental and numerical methods

Analyzing the influence of temperature on the concentration of MTHPA, it can see that the higher the temperature was, the higher the conversion rate was. The comparison between the experimental results and the numerical simulation showed that the reaction rate was seriously reduced when the temperature was lower than 65 °C, and the residual MA will lead to the subsequent steps of vacuum distillation. The reaction time was 8 min. The minimal difference between the experimental results and the numerical simulation may be due to the simplification of the solvent and the fluctuation of temperature and pressure, but this can be the best reaction time. For the study parameter of D-A reaction calculation, only conversion rate was selected, because polymerization did not occur during continuous flow capillary reactor experiment. Therefore, the selectivity of 100 % can be defined for D-A reactions with pressure of 0.3 MPa.

4. Conclusion

In the experiment, we compared the effect of MTHPA synthesis in kettle and continuous flow capillary reactor. [53] It was found that the

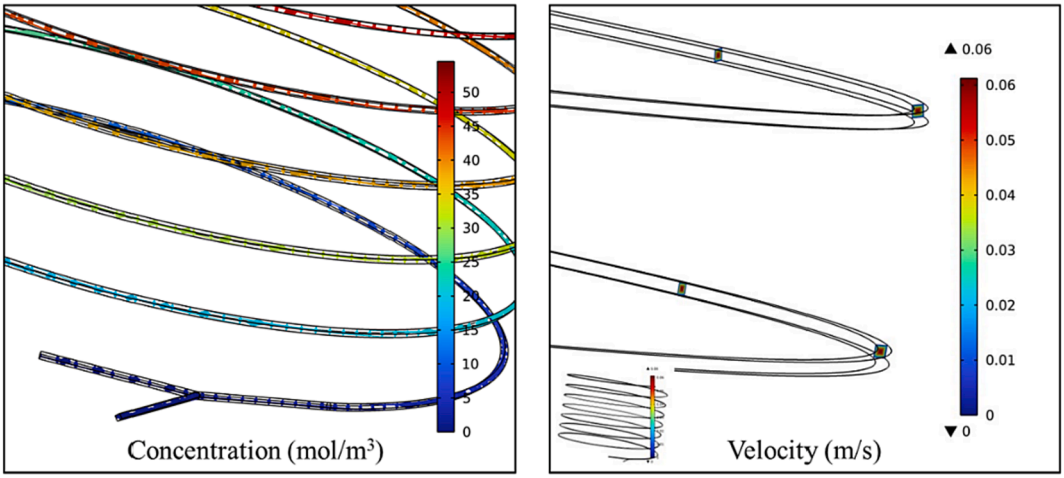

Fig. 11. MTHPA concentration distribution and fluid velocity distribution.

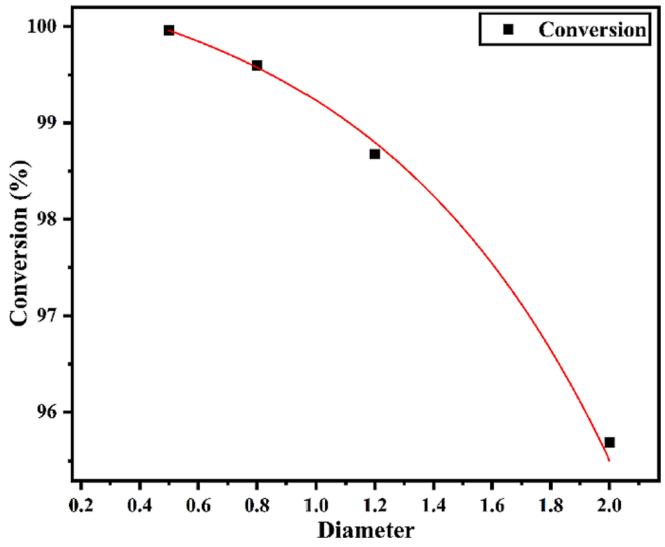

Fig. 12. Simulation of the effect of radius on D-A reaction.

optimum temperature of kettle synthesis was 65 °C, the optimum time was 30 min, and the C_5/MA raw material ratio was 1.08. At the same temperature, continuous flow capillary reactor greatly increased the conversion and shortened the reaction time to 8 min. The influence of micro size on the synthesis reaction was also examined. The conversion of D-A synthesis in circular tubes with diameters of 0.5 mm and 0.8 mm was 100 %, much better than that in 1.2 mm and 2.0 mm tubes. In order to maintain a homogeneous reaction system, we used Aspen simulation to obtain the optimal system pressure of 0.3 MPa, which prevents the occurrence of self polymerization side reactions during the vaporization of diene.Most importantly, we used Comsol simulation software to explain the experimental phenomenon, and based on the modeling results obtained by accurate dynamic parameters, it was determined that the changing trend of the influencing factors of the microchannel in the D-A reaction process was consistent with the experimental phenomenon. The polymerization reaction was ignored in the simulation process. However, the conversion rate at 65 °C and 8 min is 99 %, which is consistent with the experimental results. Therefore, microchannels can avoid the occurrence of side reactions in the industrial synthesis of MTHPA, which has a good application prospect.

CRediT authorship contribution statement

Lei Yin: Writing – original draft. **Tingting Ge:** Formal analysis. **Cuncun Zuo:** Writing – review & editing. **Ming Wang:** Formal analysis. **Guangjun Cui:** Formal analysis. **Yuchao Li:** Visualization. **Haofei Huang:** Writing – review & editing, Funding acquisition. **Liping Zhang:** Formal analysis.

Declaration of competing interest

The authors declare that they have no known competing financial interests or personal relationships that could have appeared to influence the work reported in this paper.

Acknowledgment

The authors express their gratitude to the National Natural Science Foundation of China (22178200), the Natural Science Foundation of Shandong Province, China (ZR2019MB038), Science and Technology Support Plan for Youth Innovation of Colleges and Universities of Shandong Province of China (2019KJC030), Shandong Province science and technology smes innovation ability improvement project (2022TSGC2283), and also thank the support of construction funds of Project of Yellow River Delta Research Institute (2020) and Zibo Lu Hua Hong Jin New Materials Research Institute.

Appendix A. Supplementary data

Supplementary data to this article can be found online at https://doi.org/10.1016/j.arabjc.2024.105696.

References

Abid, M.A., Kadhim, D.A., 2020. Novel comparison of iron oxide nanoparticle preparation by mixing iron chloride with henna leaf extract with and without applied pulsed laser ablation for methylene blue degradation. J. Environ. Chem. Eng. 8, 104138 https://doi.org/10.1016/j.jece.2020.104138.

Abid, M.A., Kadhim, D.A., 2022. Synthesis of iron oxide nanoparticles by mixing chilli with rust iron extract to examine antibacterial activity. Mater. Technol. 37, 1494–1503. https://doi.org/10.1080/10667857.2021.1959189.

Abideen, Z.U., Teng, F., Gu, W., Yang, Z., Zhang, A., Zhao, F., Shah, A.H., 2020. Enhanced visible light photocatalytic activity of CeO2@Zn0.5Cd0.5S by facile CE (IV)/CE(III) cycle. Arab. J. Chem. 13, 4198–4209. https://doi.org/10.1016/j.arabjc.2019.06.013.

Abiev, R.S., Pavlyukova, Y.N., Nesterova, O.M., Svetlov, S.D., Ostrovskii, V.A., 2019. Mass transfer intensification of 2-methyl-5-nitrotetrazole synthesis in two-phase liquid–liquid Taylor flow in microreactor. Chem. Eng. Res. Des. 144, 444–458. https://doi.org/10.1016/j.cherd.2019.01.033.

Aguilar, R., Santoyo, B.M., Zárate-Zárate, D., Vázquez, M.A., Padilla, R.M., Jiménez-Vázquez, H.A., Tamariz, J., 2020. Stereoselectivity of the captodative alkenes 1-

acetylvinyl arenecarboxylates in diels-Alder reactions with cyclic dienes and stereospecific rearrangement of their bicyclo[2.2.n] α-ketol adducts. Arab. J. Chem. 13, 900–915. https://doi.org/10.1016/j.arabjc.2017.08.008.

Asano, S., Yatabe, S., Maki, T., Mae, K., 2019. Numerical and experimental quantification of the performance of microreactors for scaling-up fast chemical reactions. Org. Process Res. Dev. 23, 807–817. https://doi.org/10.1021/acs.oprd.8b00356.

Barabanova, A.I., Lokshin, B.V., Kharitonova, E.P., Afanasyev, E.S., Askadskii, A.A., Philippova, O.E., 2019. Curing cycloaliphatic epoxy resin with 4-methylhexahydrophthalic anhydride: catalyzed vs. uncatalyzed reaction. Polymer (guildf). 178, 121590 https://doi.org/10.1016/j.polymer.2019.121590.

Briou, B., Améduri, B., Boutevin, B., 2021. Trends in the diels-Alder reaction in polymer chemistry. Chem. Soc. Rev. 50, 11055–11097. https://doi.org/10.1039/D0CS01382J.

Cao, Y., Noël, T., 2019. Efficient electrocatalytic reduction of furfural to furfuryl alcohol in a microchannel flow reactor. Org. Process Res. Dev. 23, 403–408. https://doi.org/10.1021/acs.oprd.8b00428.

Chen, X., Wang, X., Wang, S., Qi, J., Xie, K., Liu, X., Li, J., 2017. Furfuryl alcohol functionalized graphene for sorption of radionuclides. Arab. J. Chem. 10, 837–844. https://doi.org/10.1016/j.arabjc.2016.06.009.

De Oliveira, P.H.R., Bruno, B.M., Leão, R.A.C., Miranda, L.S.M., San Gil, R.A.S., de Souza, R.O.M.A., Finelli, F.G., 2019. From immobilization to catalyst use: a complete continuous-flow approach towards the use of immobilized organocatalysts. ChemCatChem 11, 5553–5561. https://doi.org/10.1002/cctc.201901129.

De Oliveira, G.X., Lira, J.O.B., Cambié, D., Noël, T., Riella, H.G., Padoin, N., Soares, C., 2020. CFD analysis of a luminescent solar concentrator-based photomicroreactor (LSC-PM) with feedforward control applied to the synthesis of chemicals under fluctuating light intensity. Chem. Eng. Res. Des. 153, 626–634. https://doi.org/10.1016/j.cherd.2019.10.047.

De Risi, C., Bortolini, O., Brandolese, A., Di Carmine, G., Ragno, D., Massi, A., 2020. Recent advances in continuous-flow organocatalysis for process intensification. React. Chem. Eng. 5, 1017–1052. https://doi.org/10.1039/d0re00076k.

Deng, Q., Lei, Q., Shen, R., Chen, C., Zhang, L., 2017. The continuous kilogram-scale process for the synthesis of 2,4,5-trifluorobromobenzene via gattermann reaction using microreactors. Chem. Eng. J. 313, 1577–1582. https://doi.org/10.1016/j.cej.2016.11.035.

Fedyaeva, O.N., Artamonov, D.O., Vostrikov, A.A., 2019. Heterogeneous–homogeneous oxidation of pyrrole in water vapor at elevated pressure. Combust. Flame 210, 183–192. https://doi.org/10.1016/j.combustflame.2019.08.029.

Fu, W.C., Macqueen, P.M., Jamison, T.F., 2021. Continuous flow strategies for using fluorinated greenhouse gases in fluoroalkylations. Chem. Soc. Rev. 50, 7378–7394. https://doi.org/10.1039/d0cs00670j.

Girish, Y.R., Pandit, S., Pandit, S., De, M., 2017. Graphene oxide as a carbocatalyst for a diels-Alder reaction in an aqueous medium. Chem. - an Asian J. 12, 2393–2398. https://doi.org/10.1002/asia.201701072.

Hou, X., Song, C., Ma, Z., Chen, B., Zhao, L., Huang, J., Yuan, E., Cui, T., 2022. paUniversality analysis of the reactionthway and product distribution in C5–C10 n-alkanes pyrolysis. J. Anal. Appl. Pyrolysis 162, 105451. https://doi.org/10.1016/j.jaap.2022.105451.

Inoue, T., Ohtaki, K., Murakami, S., Matsumoto, S., 2013. Direct synthesis of hydrogen peroxide based on microreactor technology. Fuel Process. Technol. 108, 8–11. https://doi.org/10.1016/j.fuproc.2012.04.009.

Ion, I., Faïçal, L., 2023. Direct-air capture conversion of CO_2 in fixed-bed microreactors with immobilized formate dehydrogenase and glucose dehydrogenase: concept feasibility. Chem. Eng. Res. Des. 193, 306–319. https://doi.org/10.1016/j.cherd.2023.03.031.

Jean, C.G.d.S., José, L.F.A., Guilherme, D.M., Michele, D.D., 2023. Photocatalytic degradation of ethylene in tubular microreactor coated with thin-film of TiO_2: mathematical modeling with experimental validation and geometry analysis using computational fluid dynamics simulations. Chem. Eng. Res. Des. 196, 101–117. https://doi.org/10.1016/j.cherd.2023.06.036.

Jing, Z., Ge, T., Guo, H., Li, Y., Li, Z., Zuo, C., Wang, M., Huang, H., Guo, L., Cui, G., 2023. Experimental study on diels-Alder addition of conjugated dienes directly from cracking C_5 fraction by continuous micro-channel reactors. Fuel. 349, 128699 https://doi.org/10.1016/j.fuel.2023.128699.

Kadhim, D.A., Muslim, A.A., Salih, W.M., 2024. Development of iron oxide nanoparticles using egg peel (brown) extract as a useful tool for removing the MB dye. Mat Sci Eng B-Adv. 300, 117104 https://doi.org/10.1016/j.mseb.2023.117104.

Liu, Y., Yao, C., Chen, G., 2022. Gas–liquid–liquid slug flow and mass transfer in hydrophilic and hydrophobic microreactors. Chinese J. Chem. Eng. 50, 85–94. https://doi.org/10.1016/j.cjche.2022.07.023.

Ma, Y., Zhu, W., Benton, M.G., Romagnoli, J., 2019. Continuous control of a polymerization system with deep reinforcement learning. J. Process Control 75, 40–47. https://doi.org/10.1016/j.jprocont.2018.11.004.

Medrán, N.S., Dezotti, F., Pellegrinet, S.C., 2019. Remarkable reactivity of boron-substituted furans in the diels-Alder reactions with maleic anhydride. Org. Lett. 21, 5068–5072. https://doi.org/10.1021/acs.orglett.9b01662.

Mizuno, K., Nishiyama, Y., Ogaki, T., Terao, K., Ikeda, H., Kakiuchi, K., 2016. Utilization of microflow reactors to carry out synthetically useful organic photochemical reactions. J. Photochem. Photobiol. C Photochem. Rev. 29, 107–147. https://doi.org/10.1016/j.jphotochemrev.2016.10.002.

Nguyen, T.S., Hoang, N.H., Hussain, M.A., Tan, C.K., 2019. Tracking-error control via the relaxing port-hamiltonian formulation: application to level control and batch polymerization reactor. J. Process Control 80, 152–166. https://doi.org/10.1016/j.jprocont.2019.05.014.

Pennemann, H., Watts, P., Haswell, S.J., Hessel, V., Löwe, H., 2004. Benchmarking of microreactor applications. Org. Process Res. Dev. 8, 422–439. https://doi.org/10.1021/op0341770.

Pontes, P.C., Chen, K., Naveira-Cotta, C.P., Costa Junior, J.M., Tostado, C.P., Quaresma, J.N.N., 2016. Mass transfer simulation of biodiesel synthesis in microreactors. Comput. Chem. Eng. 93, 36–51. https://doi.org/10.1016/j.compchemeng.2016.05.010.

Russo, D., Di Somma, I., Marotta, R., Tomaiuolo, G., Andreozzi, R., Guido, S., Lapkin, A. A., 2017. Intensification of nitrobenzaldehydes synthesis from benzyl alcohol in a microreactor. Org. Process Res. Dev. 21, 357–364. https://doi.org/10.1021/acs.oprd.6b00426.

Saeedi, I.A., Andritsch, T., Vaughan, A.S., 2019. On the dielectric behavior of amine and anhydride cured epoxy resins modified using multi-terminal epoxy functional network modifier. Polymers (basel). 11 https://doi.org/10.3390/polym11081271.

Sagandira, C.R., Siyawamwaya, M., Watts, P., 2020. 3D printing and continuous flow chemistry technology to advance pharmaceutical manufacturing in developing countries. Arab. J. Chem. 13, 7886–7908. https://doi.org/10.1016/j.arabjc.2020.09.020.

Salih, W.M., Sabah, R., Kadhim, D.A., Kadhum, H.A., Abid, M.A., 2024. Green synthesis of (CeO2)-(CuO) nanocomposite, analytical study, and investigation of their anticancer activity against Saos-2 osteosarcoma cell lines. Inorg Chem Commun. 159, 111730 https://doi.org/10.1016/j.inoche.2023.111730.

Santana, H.S., Tortola, D.S., Reis, É.M., Silva, J.L., Taranto, O.P., 2016. Transesterification reaction of sunflower oil and ethanol for biodiesel synthesis in microchannel reactor: experimental and simulation studies. Chem. Eng. J. 302, 752–762. https://doi.org/10.1016/j.cej.2016.05.122.

Sheehan, M.E., Sharratt, P.N., 1998. Molecular dynamics methodology for the study of the solvent effects on a concentrated diels-Alder reaction and the separation of the post-reaction mixture. Comput. Chem. Eng. 22, 27–33. https://doi.org/10.1016/s0098-1354(98)00035-0.

Shuai, G., Le-wu, Z., Guang-kai, Z., Xin-guang, W., Bin-dong, L., 2022. Scale-up and development of synthesis 2-ethylhexyl nitrate in microreactor using the box-behnken design. Org. Process Res. Dev. 1, 174–182. https://doi.org/10.1021/acs.oprd.1c00388.

Ul Abideen, Z., Teng, F., 2018. Enhanced photochemical activity and stability of ZnS by a simple alkaline treatment approach. CrystEngComm 20, 7866–7879. https://doi.org/10.1039/c8ce01417e.

Wan, Y., Guo, W., Xiao, J., Yan, D., Zhao, X., Guo, S., Liu, J., Zhong, Q., Yang, T., Zhao, Y., Chang, X., Gao, X., 2020. Integrated UV-based photo microreactor-distillation technology toward process intensification of continuous ultra-high-purity electronic-grade silicon tetrachloride manufacture. Chinese J. Chem. Eng. 28, 2248–2255. https://doi.org/10.1016/j.cjche.2020.06.023.

Wan, Y., Liu, J., Mao, Q., Chang, X., Song, Y., Yuan, Z., You, Z., Zhao, X., Tian, J.Z., Yan, D., Xiao, J., Zhong, Q., 2022. Exploration of photocatalytic chlorination combined simplified distillation to produce electronic grade high-purity trichlorosilane via microchannel reactor experiments, multiphase-flow simulation, ReaxFF MD, and DFT. Chem. Eng. J. 450, 138020 https://doi.org/10.1016/j.cej.2022.138020.

Wang, F., Huang, J., Xu, J., 2018. Continuous-flow synthesis of azo dyes in a microreactor system. Chem. Eng. Process. - Process Intensif. 127, 43–49. https://doi.org/10.1016/j.cep.2018.03.014.

Wang, F.J., Huang, J.P., Xu, J.H., 2019b. Continuous-flow synthesis of the azo pigment yellow 14 using a three-stream micromixing process. Org. Process Res. Dev. 23, 2637–2646. https://doi.org/10.1021/acs.oprd.9b00286.

Wang, C., Si, Z., Wu, X., Lv, W., Bi, K., Zhang, X., Chen, L., Xu, Y., Zhang, Q., Ma, L., 2019a. Mechanism study of aromatics production from furans with methanol over zeolite catalysts. J. Anal. Appl. Pyrolysis 139, 87–95. https://doi.org/10.1016/j.jaap.2019.01.013.

Wazarkar, K., Sabnis, A., 2018. Cardanol based anhydride curing agent for epoxy coatings. Prog. Org. Coatings 118, 9–21. https://doi.org/10.1016/j.porgcoat.2018.01.018.

Yan, B.H., Wang, C., Li, L.G., 2020. The technology of micro heat pipe cooled reactor: a review. Ann. Nucl. Energy 135. https://doi.org/10.1016/j.anucene.2019.106948.

Yedala, N., Kaisare, N.S., 2021. A CFD study of ignition of lean propane-air mixtures in a heat recirculating U-bend catalytic microreactor. Chem. Eng. Res. Des. 173, 15–26. https://doi.org/10.1016/j.cherd.2021.06.019.

Yin, L., Li, H., Ge, T., Li, Y., Zuo, C., Wang, M., Cui, G., Huang, H., Guo, L., 2023. Continuous heterogeneous isomerization of 3/4-methyltetrahydrophthalic anhydride (3/4-MTHPA) with acid-and base-modified γ-Al2O3 catalysts. New. J. Chem. https://doi.org/10.1039/D2NJ05002A.

Yuichi, N., Brian, A.M., Yutaka, M., 2022. Antibody-drug conjugate synthesis using continuous flow microreactor technology. Org. Process Res. Dev. 9, 2766–2770. https://doi.org/10.1021/acs.oprd.2c00217.

Yun, L., Zhao, J., Tang, X., Ma, C., Yu, Z., Meng, Q., 2021. Selective oxidation of benzylic sp3C-H bonds using molecular oxygen in a continuous-flow microreactor. Org. Process Res. Dev. 25, 1612–1618. https://doi.org/10.1021/acs.oprd.1c00080.

Zhang, Y., Li, M., Wen, J., Liu, X., Dou, B., Jiang, Y., 2023. Preparation of polyaniline encapsulated acrylic resin microcapsules and its active corrosion protection of coating for magnesium alloy. Arab. J. Chem. 16, 105129 https://doi.org/10.1016/j.arabjc.2023.105129.

Zhang, A., Teng, F., Zhang, Q., Zhai, Y., Liu, Z., Liu, Z., Gu, W., Hao, W., Abideen, Z.U., Teng, Y., 2018. Boosted electrochemistry properties of Cu4[(OH)0.29Cl0.71](OH)6 hexagonal prisms by 3D-cage atomic configuration of (100) facet. Appl. Surf. Sci. 428, 586–592. https://doi.org/10.1016/j.apsusc.2017.09.182.

Zhou, Y., Zhang, J., Baral, A., Ju, S., Gu, Y., 2022. High-efficiency absorption of low NOX concentration in metallurgical flue gas using a three dimensional printed large-flow

microstructured reactor. Arab. J. Chem. 15, 103711 https://doi.org/10.1016/j.arabjc.2022.103711.